Scattering and sublimation: A multi-scale view of μm-sized dust in the inclined disc of HD 145718

C L Davies, E A Rich, T J Harries, J D Monnier, A S E Laws, S M Andrews, J Bae, D J Wilner, N Anugu, J Ennis, T Gardner, S Kraus, A Labdon, J-B le Bouquin, C Lanthermann, G H Schaefer, B R Setterholm, T ten Brummelaar
& the G-LIGHTS collaboration

Star Formation: From Clouds to Discs – A Tribute to the Career of Lee Hartmann

October 20th 2021

Claire L. Davies

(she/her)

Post-doctoral Researcher
Astrophysics Group
University of Exeter

c.davies3@exeter.ac.uk

@cldaviesastro

cldaviesastro.github.io

UNIVERSITY OF EXETER

G-LIGHTS: Q_ϕ gallery

- Gemini Large Imaging with Gpi: Herbig/T-Tauri Survey

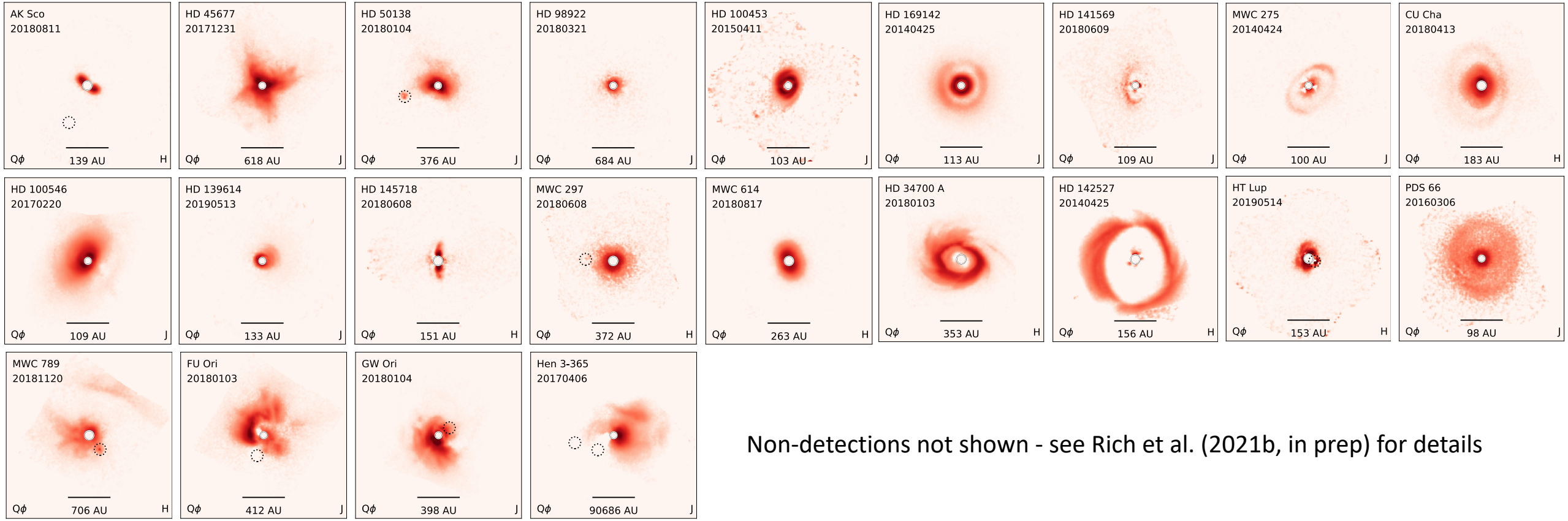

Non-detections not shown - see Rich et al. (2021b, in prep) for details

- Monnier et al. (2017, ApJ, 838, 20); Monnier et al. (2019, ApJ, 872, 122); Laws et al. (2020, ApJ, 888, 7); Rich et al. (2021a, ApJ, 913, 138); Kraus et al. (2020, Science, 369, 1233)

Inspecting HD 145718

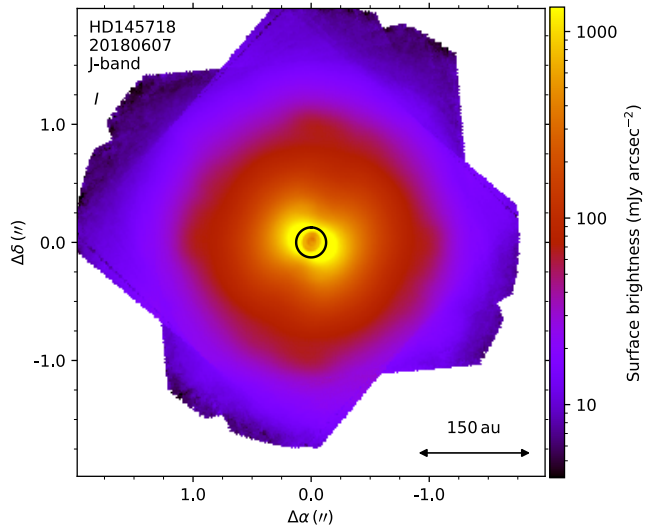

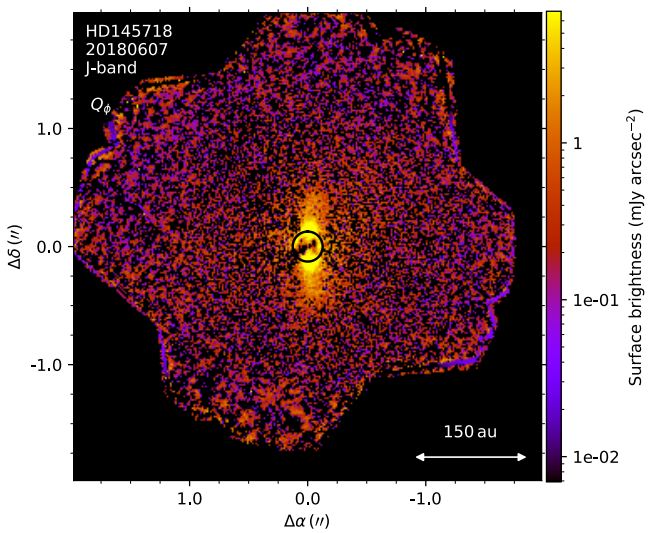

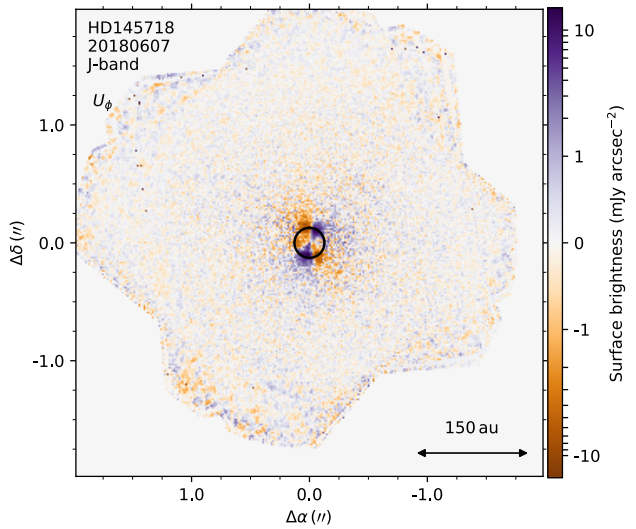

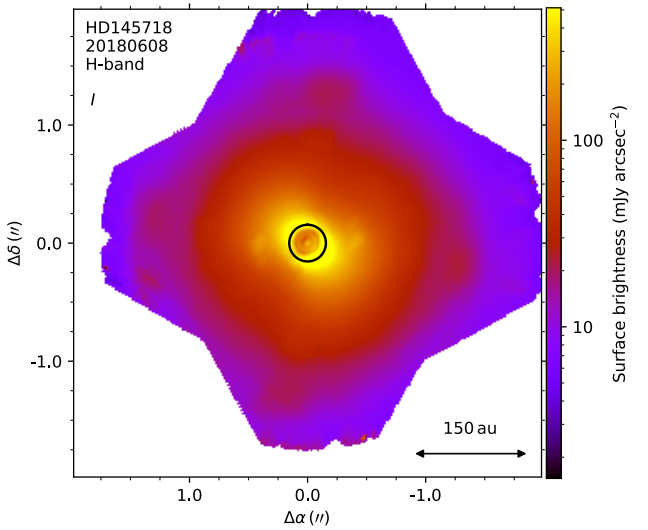

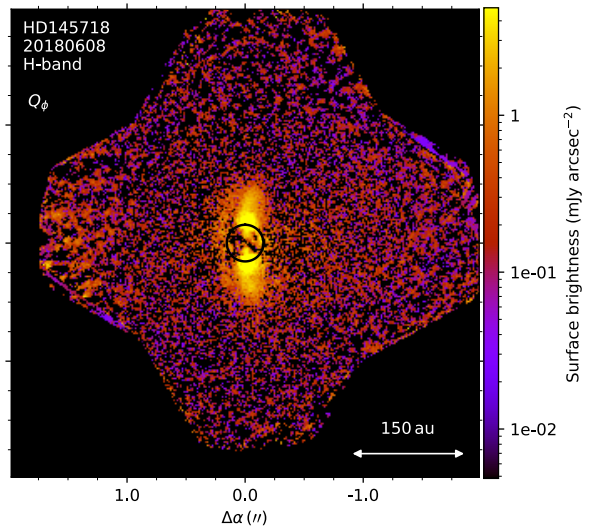

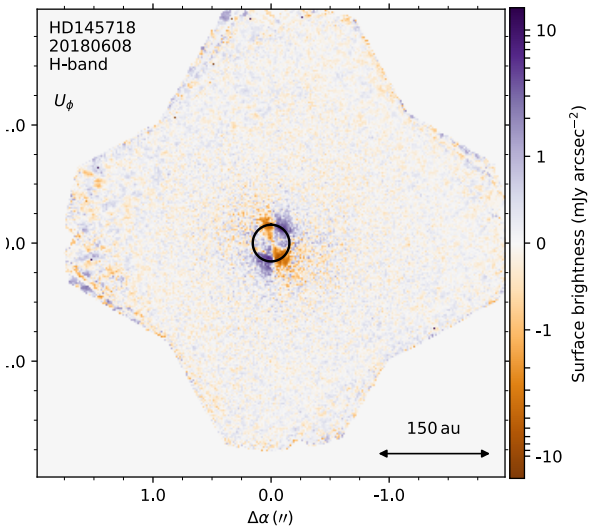

$$Q_\phi = -U\sin(2\phi) \\ -Q\cos(2\phi)$$

$$U_\phi = Q\sin(2\phi) \\ -U\cos(2\phi)$$

where

$$\phi = \tan^{-1}\left(\frac{Y - Y_0}{X - X_0}\right) \\ +\gamma$$

Davies et al. (2021, *submitted*)

Inspecting HD 145718: U_ϕ image

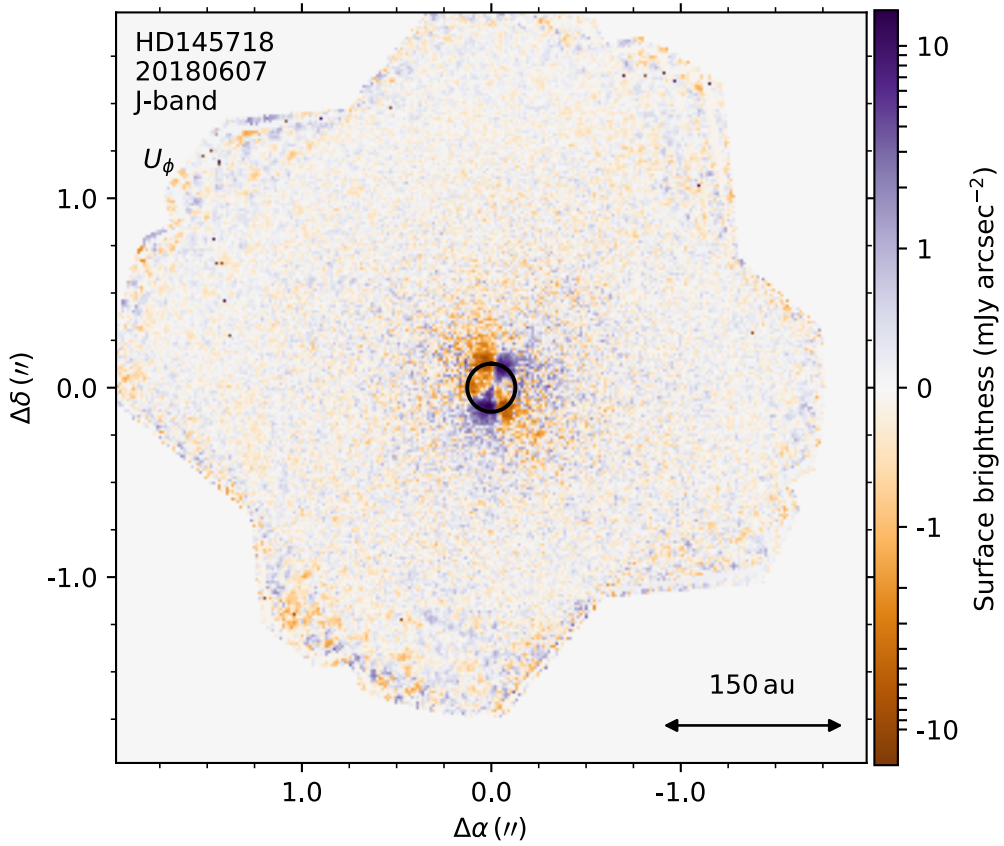

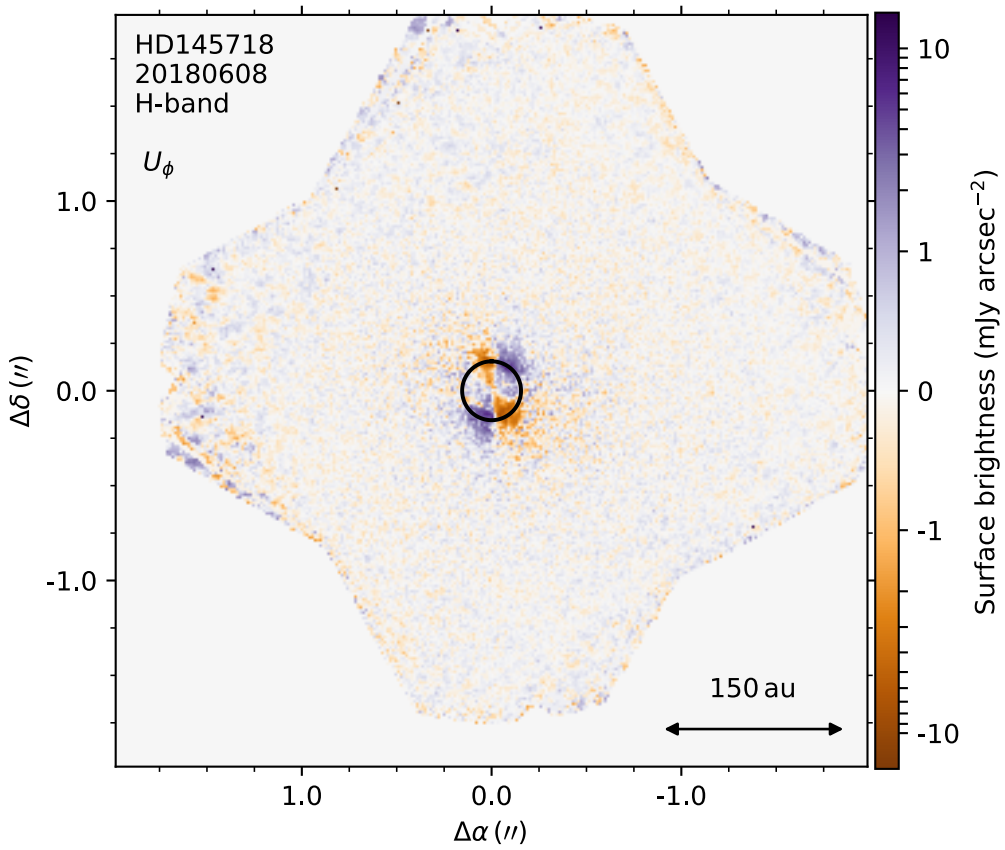

Davies et al. (2021, *submitted*)

Inspecting HD 145718: Q_ϕ image

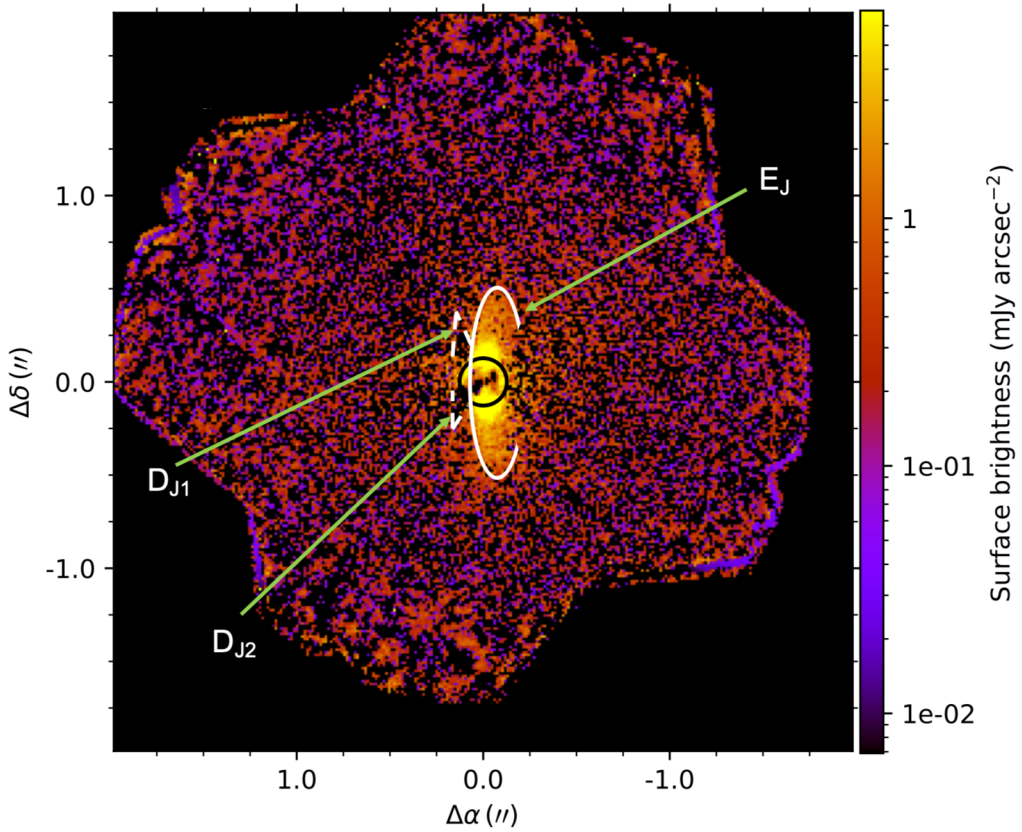

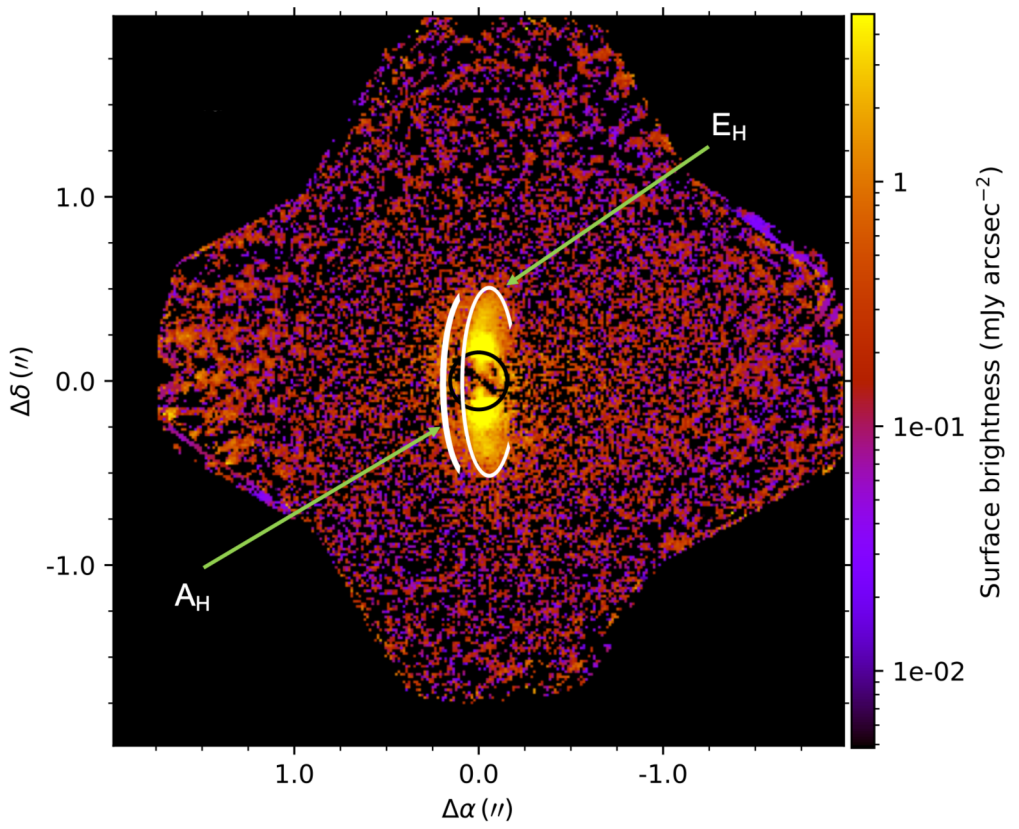

Davies et al. (2021, *submitted*)

Study motivation: HD 145718

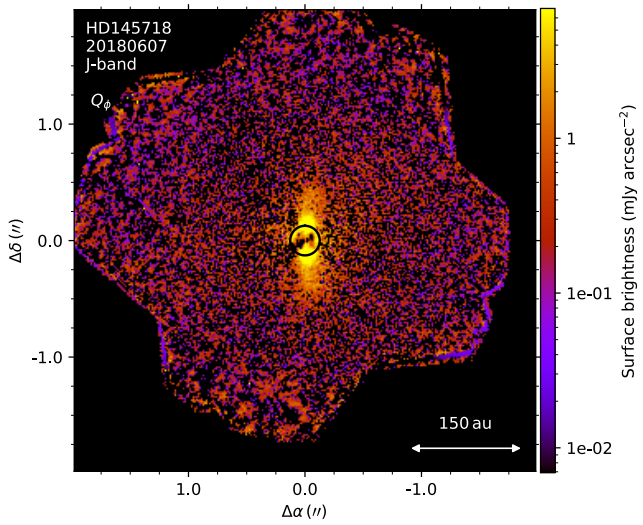

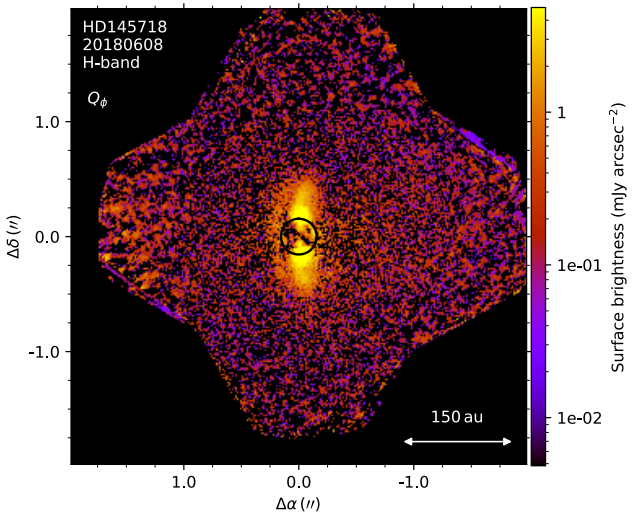

Previous H-band VLTI/PIONIER images (reconstructed from interferometry)

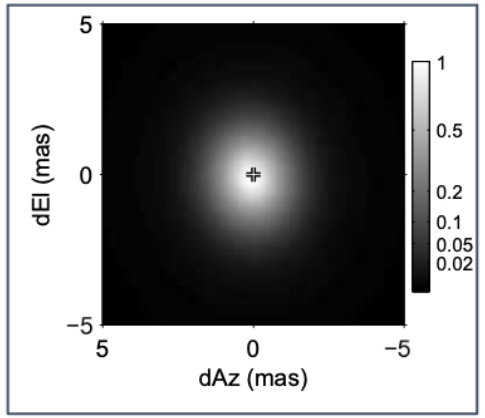

Lazareff et al. (2017, A&A, 599, 85)

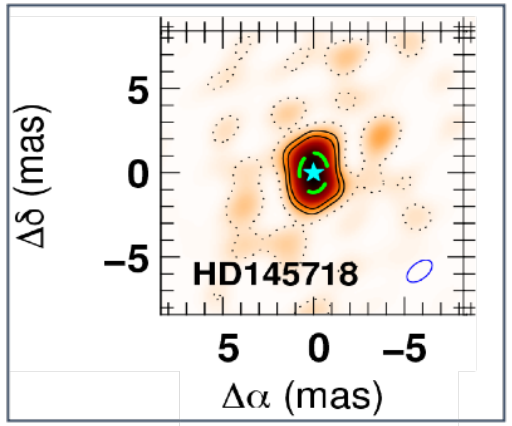

Kluska et al. (2020, A&A, 636, 116)

Previous ALMA band 6 (λ = 1.3mm) image (reconstructed from interferometric observations)

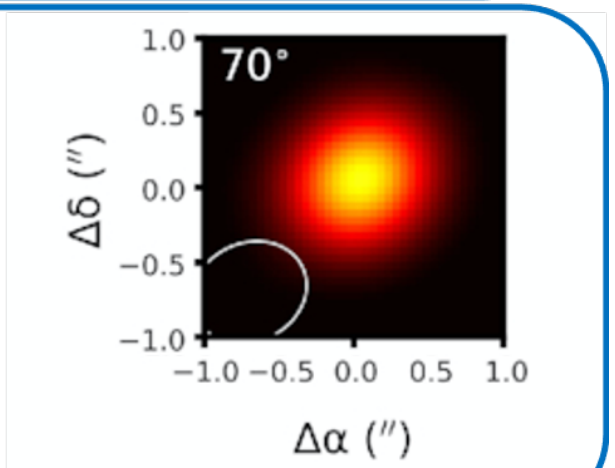

Ansdell et al. (2020, MNRAS 492, 572)

Study motivation: disc structure

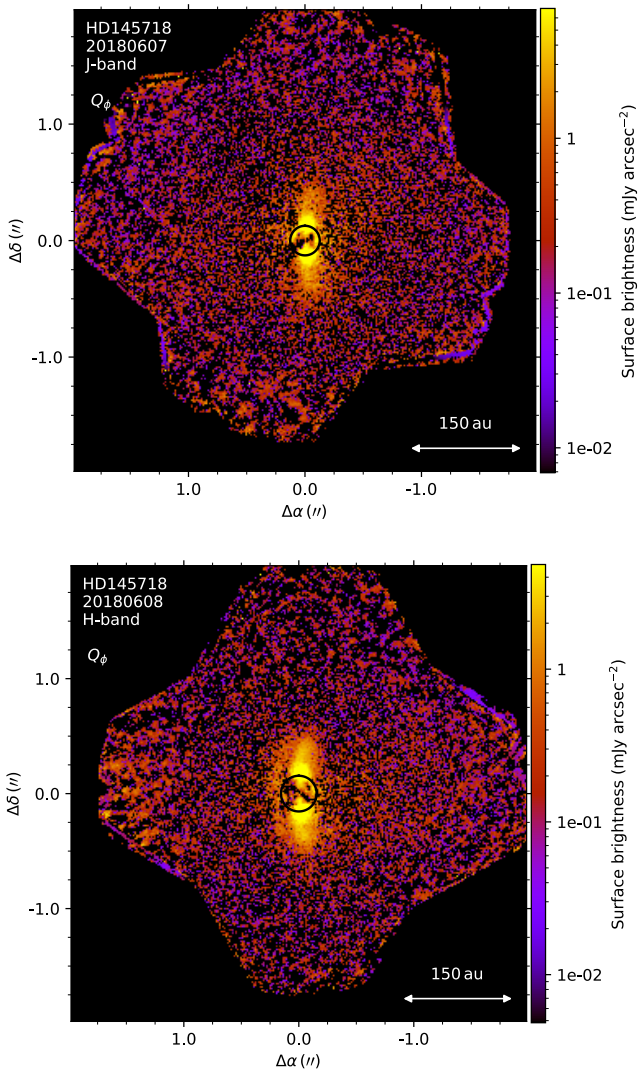

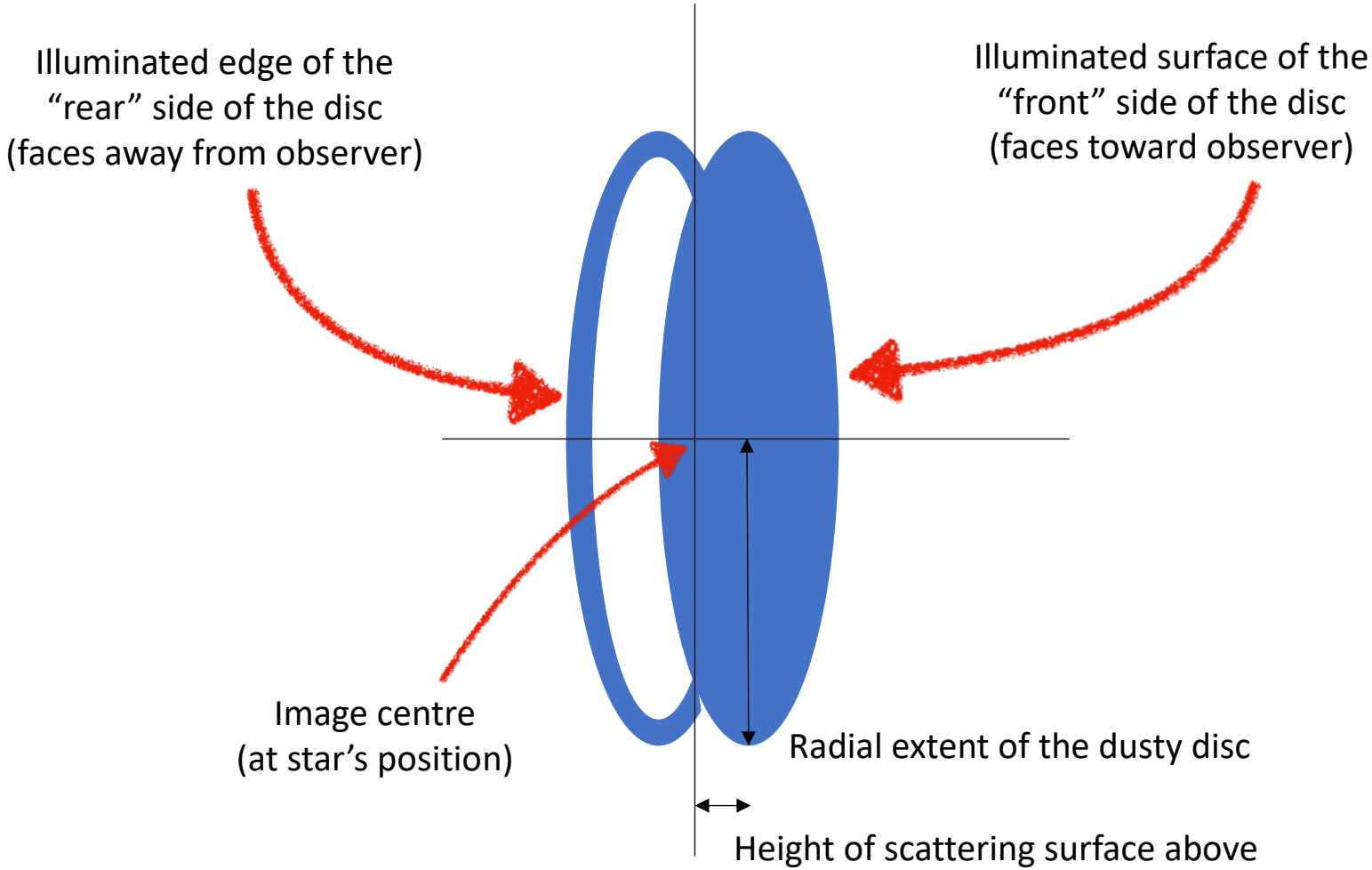

Q_ϕ Surface Brightness Isophote fitting

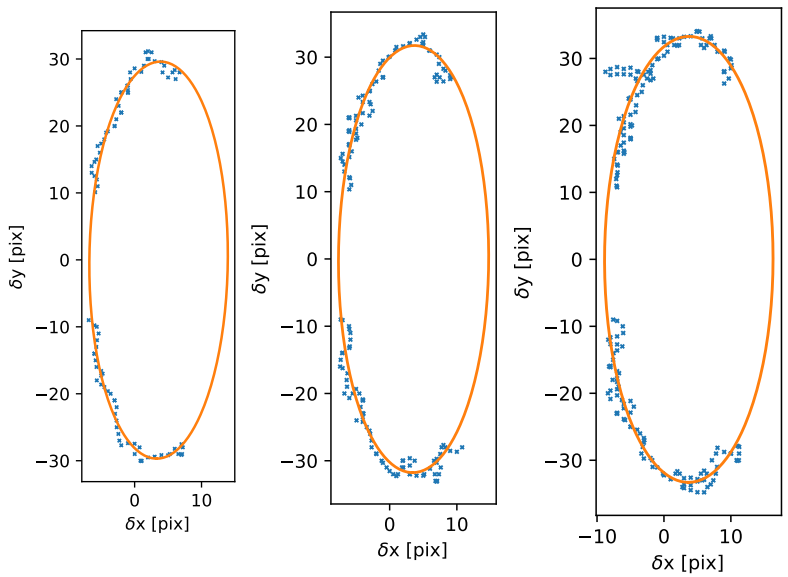

$$\mathrm{PA} = \tan^{-1}\left(\frac{\delta\,\mathrm{RA}}{\delta\,\mathrm{Dec}}\right) + \frac{\pi}{2}$$

$$h_{\mathrm{scat}}(r) = d\left((\delta\,\mathrm{RA})^2 + (\delta\,\mathrm{Dec})^2\right)^{1/2}$$

S_ν (mJy/arcsec^2) (1)	r (au) (2)	i (°) (3)	PA (°) (4)	$h_{\mathrm{scat}}(r)$ (au) (5)
		J-band		
0.70	$71.4^{+0.6}_{-0.6}$	$68.1^{+0.6}_{-0.7}$	$-0.7^{+0.3}_{-0.4}$	$9.5^{+0.4}_{-0.4}$
0.75	$71.0^{+0.6}_{-0.6}$	$68.3^{+0.7}_{-0.7}$	$-0.5^{+0.3}_{-0.4}$	$9.6^{+0.5}_{-0.4}$
0.80	$70.7^{+0.6}_{-0.6}$	$68.2^{+0.7}_{-0.7}$	$-0.6^{+0.3}_{-0.4}$	$9.8^{+0.5}_{-0.5}$
0.85	$69.5^{+0.6}_{-0.6}$	$67.1^{+0.7}_{-0.7}$	$-0.1^{+0.3}_{-0.4}$	$10.3^{+0.5}_{-0.5}$
0.90	$69.1^{+0.7}_{-0.6}$	$66.9^{+0.8}_{-0.9}$	$-0.6^{+0.4}_{-0.5}$	$10.8^{+0.6}_{-0.5}$
0.95	$66.9^{+0.6}_{-0.6}$	$67.7^{+0.8}_{-0.9}$	$-0.1^{+0.3}_{-0.4}$	$9.2^{+0.6}_{-0.5}$
1.00	$66.6^{+0.6}_{-0.6}$	$68.4^{+0.8}_{-0.9}$	$0.3^{+0.3}_{-0.3}$	$9.0^{+0.6}_{-0.6}$
1.05	$66.0^{+0.6}_{-0.6}$	$69.0^{+0.8}_{-0.8}$	$0.6^{+0.3}_{-0.3}$	$8.5^{+0.5}_{-0.5}$
1.10	$65.4^{+0.6}_{-0.6}$	$68.6^{+0.8}_{-0.9}$	$0.2^{+0.3}_{-0.4}$	$8.8^{+0.5}_{-0.5}$
1.15	$64.7^{+0.6}_{-0.6}$	$68.6^{+0.8}_{-0.9}$	$0.2^{+0.3}_{-0.3}$	$9.1^{+0.5}_{-0.5}$
1.20	$63.6^{+0.5}_{-0.5}$	$67.8^{+0.8}_{-0.8}$	$0.1^{+0.3}_{-0.3}$	$9.4^{+0.5}_{-0.5}$
1.25	$62.9^{+0.5}_{-0.6}$	$67.8^{+0.9}_{-1.0}$	$0.2^{+0.3}_{-0.4}$	$9.4^{+0.7}_{-0.6}$

$$0.13 \leq \frac{h_{scat}(r)}{r} \leq 0.16$$

Aspect ratios consistent with findings for "gapped" discs (0.09-0.25):

- Avenhaus et al. (2018, ApJ, 863, 44)
- Ginski et al. (2016, A&A, 595, 112)

S_ν (mJy/arcsec^2) (1)	r (au) (2)	i (°) (3)	PA (°) (4)	$h_{\mathrm{scat}}(r)$ (au) (5)
		H-band		
0.80	$71.6^{+0.5}_{-0.5}$	$67.8^{+0.6}_{-0.7}$	$-0.1^{+0.3}_{-0.3}$	$8.0^{+0.5}_{-0.4}$
0.85	$71.3^{+0.4}_{-0.4}$	$68.6^{+0.5}_{-0.5}$	$-0.8^{+0.2}_{-0.3}$	$8.3^{+0.3}_{-0.3}$
0.90	$70.4^{+0.4}_{-0.4}$	$69.0^{+0.5}_{-0.5}$	$-0.7^{+0.2}_{-0.3}$	$7.7^{+0.3}_{-0.3}$
0.95	$70.0^{+0.5}_{-0.5}$	$68.6^{+0.6}_{-0.6}$	$-1.0^{+0.3}_{-0.3}$	$8.0^{+0.4}_{-0.4}$
1.00	$69.5^{+0.5}_{-0.5}$	$68.5^{+0.6}_{-0.7}$	$-1.0^{+0.3}_{-0.4}$	$8.3^{+0.4}_{-0.4}$
1.05	$69.4^{+0.4}_{-0.4}$	$69.6^{+0.5}_{-0.5}$	$-0.6^{+0.2}_{-0.3}$	$7.8^{+0.4}_{-0.4}$
1.10	$68.3^{+0.4}_{-0.4}$	$69.4^{+0.5}_{-0.5}$	$-0.3^{+0.2}_{-0.3}$	$7.7^{+0.4}_{-0.4}$
1.15	$68.2^{+0.4}_{-0.4}$	$69.4^{+0.5}_{-0.5}$	$-0.2^{+0.2}_{-0.3}$	$7.7^{+0.4}_{-0.3}$
1.20	$67.5^{+0.4}_{-0.4}$	$69.4^{+0.5}_{-0.5}$	$-0.3^{+0.2}_{-0.2}$	$7.7^{+0.4}_{-0.3}$
1.25	$67.5^{+0.4}_{-0.4}$	$68.8^{+0.5}_{-0.6}$	$-0.5^{+0.2}_{-0.3}$	$8.3^{+0.4}_{-0.4}$
1.30	$66.7^{+0.4}_{-0.4}$	$68.3^{+0.6}_{-0.7}$	$-0.6^{+0.2}_{-0.3}$	$8.5^{+0.4}_{-0.4}$
1.35	$65.6^{+0.4}_{-0.4}$	$69.9^{+0.6}_{-0.6}$	$-0.2^{+0.2}_{-0.2}$	$6.9^{+0.4}_{-0.4}$
1.40	$65.4^{+0.4}_{-0.4}$	$70.2^{+0.5}_{-0.6}$	$-0.1^{+0.2}_{-0.2}$	$7.0^{+0.4}_{-0.4}$
1.45	$65.1^{+0.4}_{-0.4}$	$70.7^{+0.5}_{-0.5}$	$-0.2^{+0.2}_{-0.2}$	$6.8^{+0.4}_{-0.4}$
1.50	$64.6^{+0.4}_{-0.4}$	$70.5^{+0.6}_{-0.6}$	$-0.4^{+0.2}_{-0.3}$	$7.0^{+0.4}_{-0.4}$
1.55	$64.5^{+0.4}_{-0.4}$	$70.4^{+0.6}_{-0.6}$	$-0.5^{+0.2}_{-0.3}$	$7.1^{+0.4}_{-0.4}$
1.60	$63.8^{+0.4}_{-0.4}$	$69.6^{+0.7}_{-0.7}$	$-0.6^{+0.3}_{-0.3}$	$7.7^{+0.5}_{-0.5}$
1.65	$62.8^{+0.4}_{-0.4}$	$69.0^{+0.7}_{-0.7}$	$-0.6^{+0.3}_{-0.3}$	$7.8^{+0.5}_{-0.5}$
1.70	$62.3^{+0.4}_{-0.4}$	$70.0^{+0.7}_{-0.8}$	$-0.7^{+0.3}_{-0.3}$	$7.0^{+0.6}_{-0.5}$
1.75	$62.1^{+0.4}_{-0.4}$	$70.0^{+0.7}_{-0.9}$	$-0.6^{+0.3}_{-0.3}$	$7.0^{+0.7}_{-0.6}$
1.80	$61.9^{+0.4}_{-0.4}$	$70.0^{+0.8}_{-0.9}$	$-0.6^{+0.3}_{-0.3}$	$7.0^{+0.7}_{-0.6}$
1.85	$61.6^{+0.5}_{-0.4}$	$69.8^{+0.8}_{-0.9}$	$-0.7^{+0.3}_{-0.3}$	$7.1^{+0.7}_{-0.7}$

$$0.10 \leq \frac{h_{scat}(r)}{r} \leq 0.13$$

Davies et al. (2021, *submitted*)

Monte Carlo Radiative Transfer modelling

TORUS (Harries 2000, MNRAS, 315, 722; Harries et al. 2019, A&C, 27, 63)

$$\rho_{\rm gas}(r,z) = \frac{\Sigma_{\rm gas}(r)}{h_{\rm gas}(r)\sqrt{2\pi}} \exp\left\{-\frac{1}{2}\left[\frac{z}{h_{\rm gas}(r)}\right]^2\right\}$$

$$h_{\rm gas}(r) = h_{0,\rm gas}\left(\frac{r}{r_0}\right)^{\beta} \quad ; \quad \Sigma_{\rm gas}(r) = \Sigma_{0,\rm gas}\left(\frac{r}{r_0}\right)^{-p}$$

see Shakura & Sunyaev (1973, A&A, 24, 337)

$$M_{\rm disc} = \frac{F_\nu d^2}{\kappa_\nu B_\nu\,(T_{\rm dust})} = 0.0097\,{\rm M}_\odot$$

Small grains:

$$T_{\rm sub,1} = G\rho_{\rm gas}^{\gamma}\,(r,z)$$

see Pollack et al. (1994, ApJ, 421, 615)

$$n(a) \propto a^{-3.5}$$

$$a_{\rm min} = 0.01\,\mu{\rm m}$$

$$0.14 \leq a_{\rm max} \leq 1.30\,\mu{\rm m}$$

see Isella & Natta (2005, A&A, 438, 899);
Davies et al. (2020, ApJ, 897, 31);
Davies & Harries (*in prep*)

Davies et al. (2021, *submitted*)

Monte Carlo Radiative Transfer modelling

TORUS (Harries 2000, MNRAS, 315, 722; Harries et al. 2019, A&C, 27, 63)

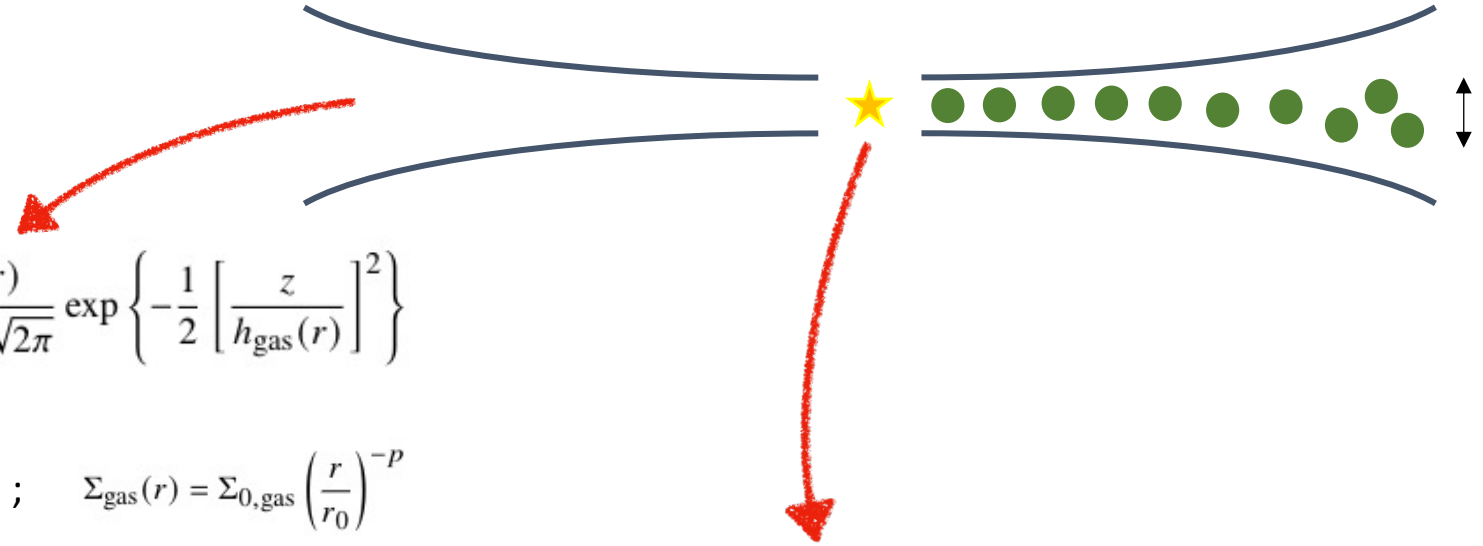

Large grains:

$T_{sub,2} = 1200$ K

$h_2 = f\ h_{\rm gas}$

$n(a) \propto a^{-3.5}$

$$\rho_{\rm gas}(r,z) = \frac{\Sigma_{\rm gas}(r)}{h_{\rm gas}(r)\sqrt{2\pi}} \exp\left\{-\frac{1}{2}\left[\frac{z}{h_{\rm gas}(r)}\right]^2\right\}$$

$$h_{\rm gas}(r) = h_{0,\rm gas}\left(\frac{r}{r_0}\right)^{\beta} \quad ; \quad \Sigma_{\rm gas}(r) = \Sigma_{0,\rm gas}\left(\frac{r}{r_0}\right)^{-p}$$

see Shakura & Sunyaev (1973, A&A, 24, 337)

$$M_{\rm disc} = \frac{F_\nu d^2}{\kappa_\nu B_\nu\,(T_{\rm dust})} = 0.0097\,{\rm M}_\odot$$

$T_{eff} = 8000$ K (Fairlamb et al. 2015, MNRAS, 453, 976); d = 152.5 pc (Gaia eDR3)

$L_\star = 14.3 L_\odot$
$A_V = 0.89$ mag
$R_\star = 1.97 R_\odot$

} Based on *BVRI* photometry from Lazareff et al. (2017, A&A, 599, 85) with R_v = 3.1

- consistent $L_\star$ found when using faint epoch photometry & R_v = 5.0 suggests a > $\lambda/2\pi$ in occulting medium

Davies et al. (2021, *submitted*)

Complementary observational data

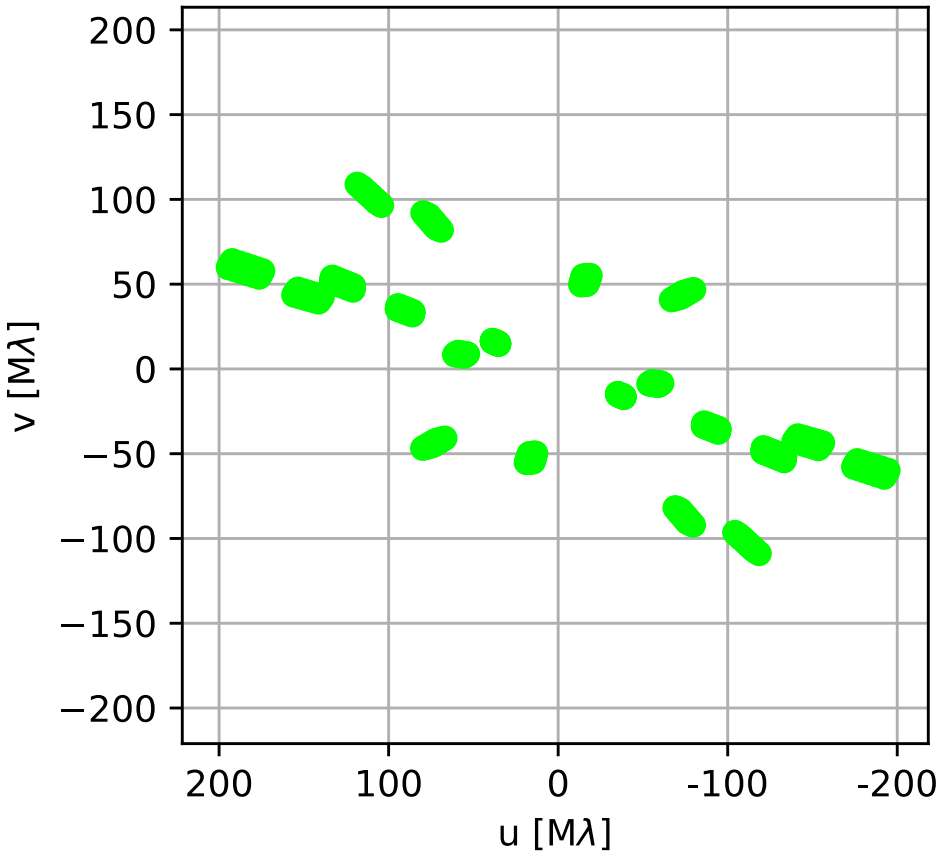

CHARA/MIRC-X

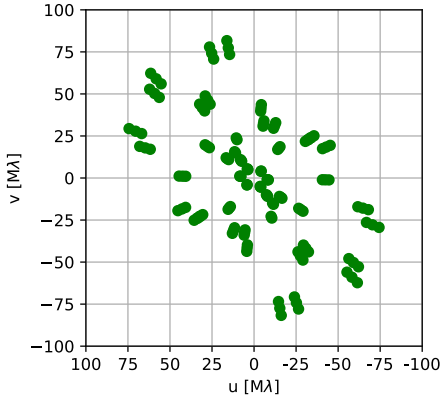

VLTI/PIONIER

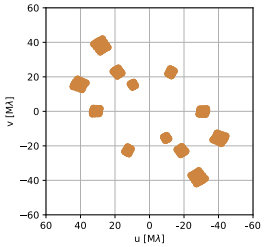

VLTI/GRAVITY

SEDBYS

SED Builder for Young Stars

Davies (2021, SoftwareX, 14, 100687)

TORUS model fitting

Parameter	Model value
$h_{0,gas}$ (au)	10
$f\,(h_{0,gas})$	0.1
β	1.15
a_{max} (μm)	0.50
R_{out} (au)	75
i (°)	72
PA (°)	0

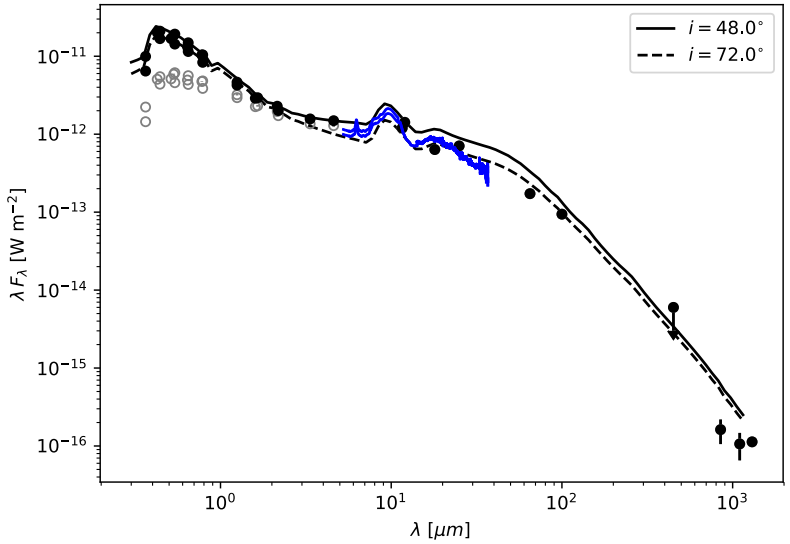

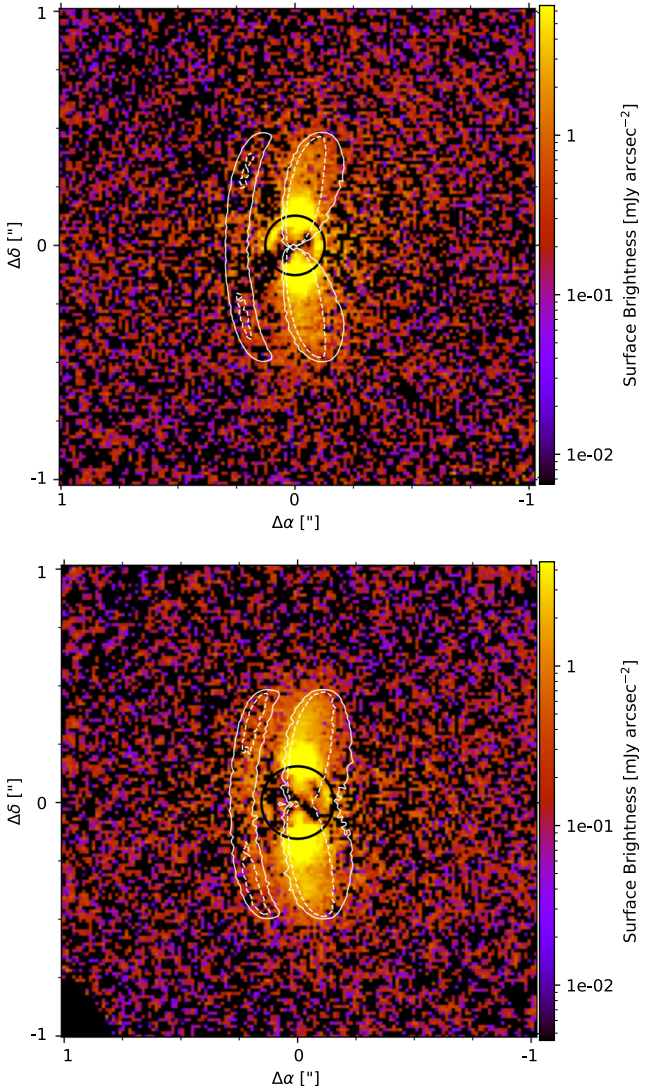

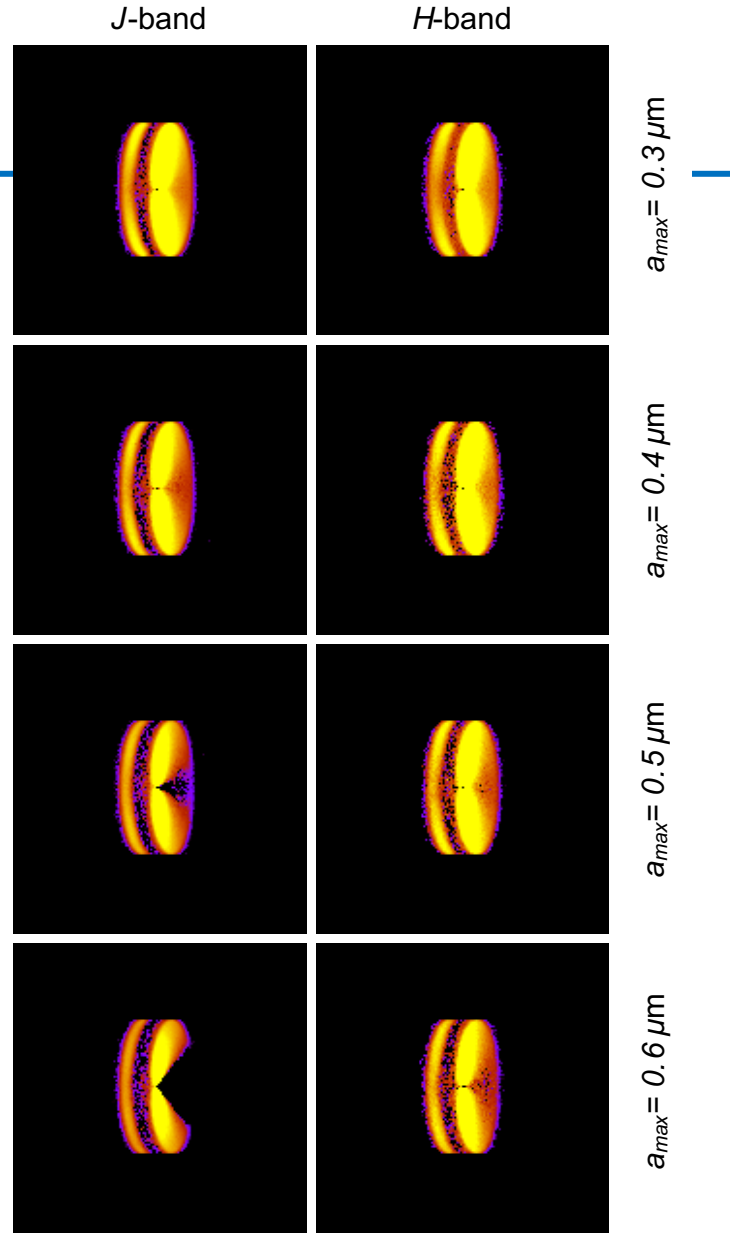

Davies et al. (2021, *submitted*)

TORUS model fitting

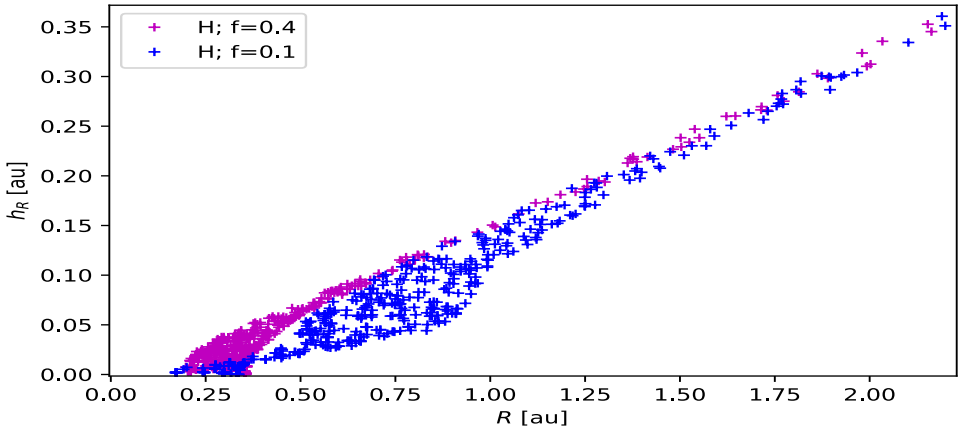

Location and extent of sublimation rim controlled by size of largest grains present: Isella & Natta (2005, A&A, 438, 899), Tannirkulam et al. (2007, ApJ, 661, 374)

Parameter	Model value
$h_{0,gas}$ (au)	10
$f(h_{0,gas})$	0.1
β	1.15
a_{max} (μm)	0.50
R_{out} (au)	75
i (°)	72
PA (°)	0

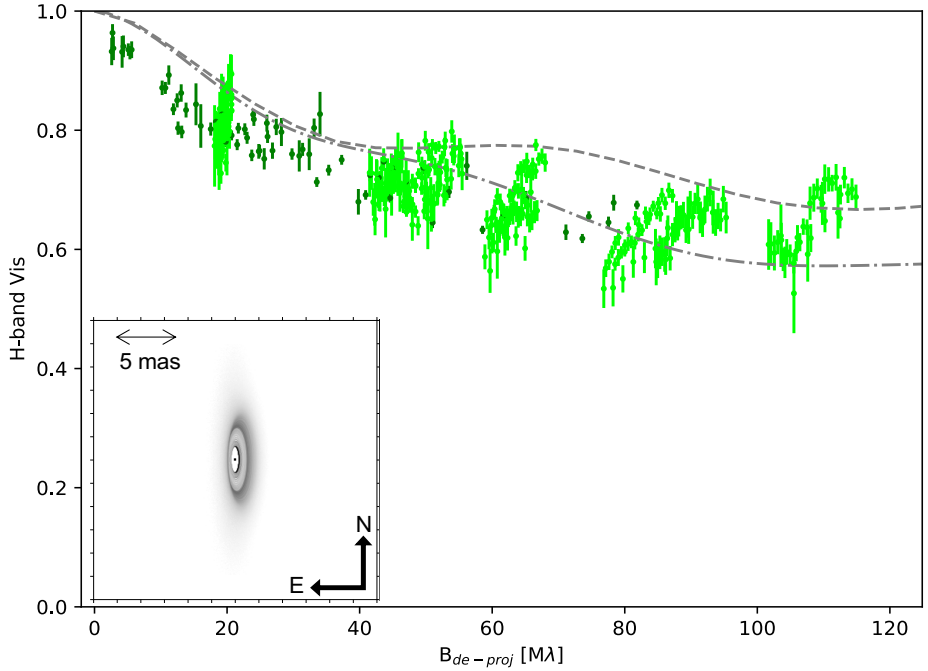

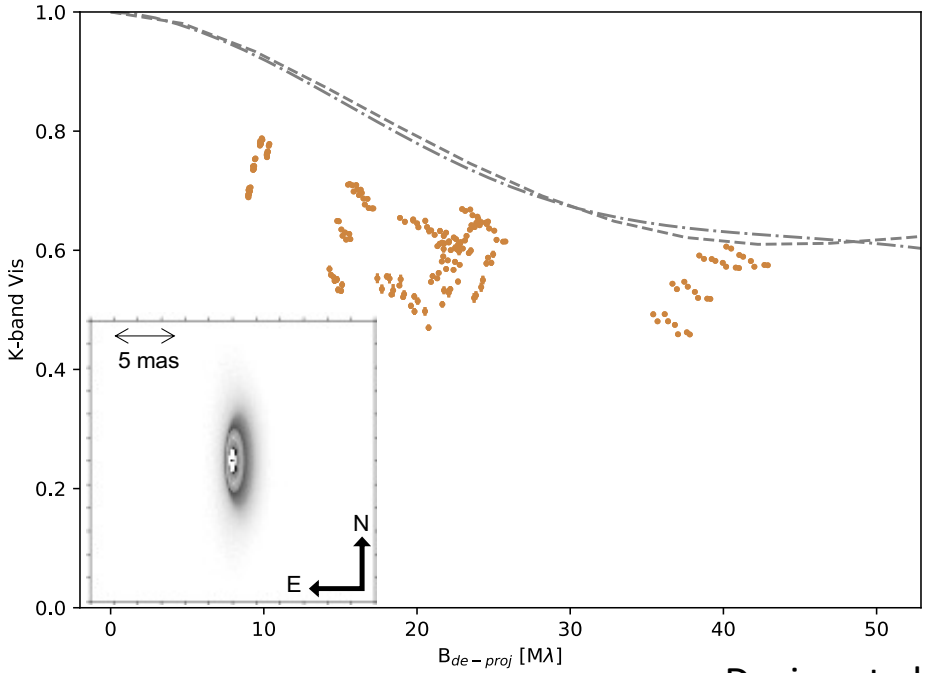

Davies et al. (2021, *submitted*)

Tests of the isophote fitting with TORUS

Scattering surface flaring from GPI data isophote fit

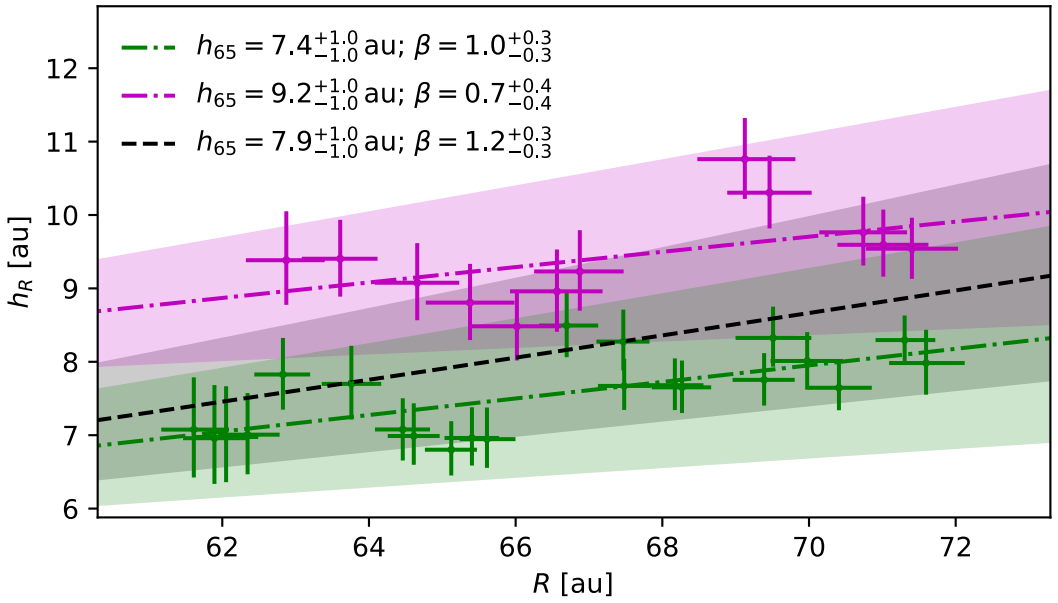

Scattering height, $h_R = h_{65}\left(\frac{r}{65\text{ au}}\right)^{\beta}$

Scattering surface flaring from TORUS model and its isophotes

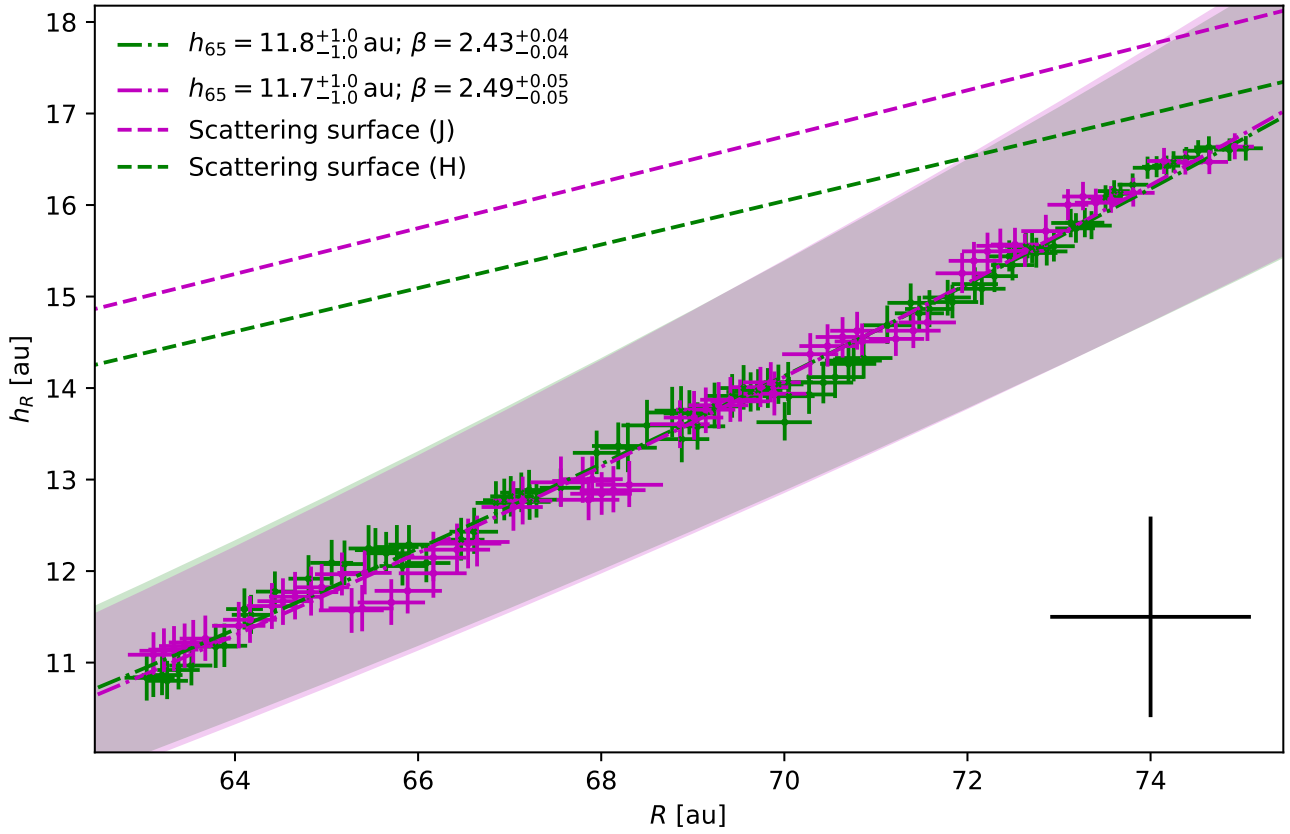

Davies et al. (2021, *submitted*)

Tests of the isophote fitting with TORUS

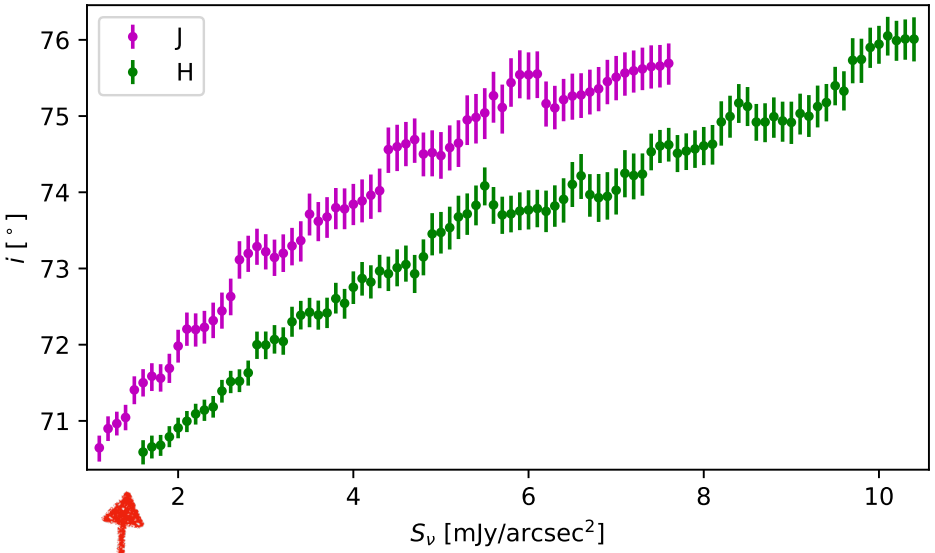

Squashed in the west due to the relative back-scattering inefficiency

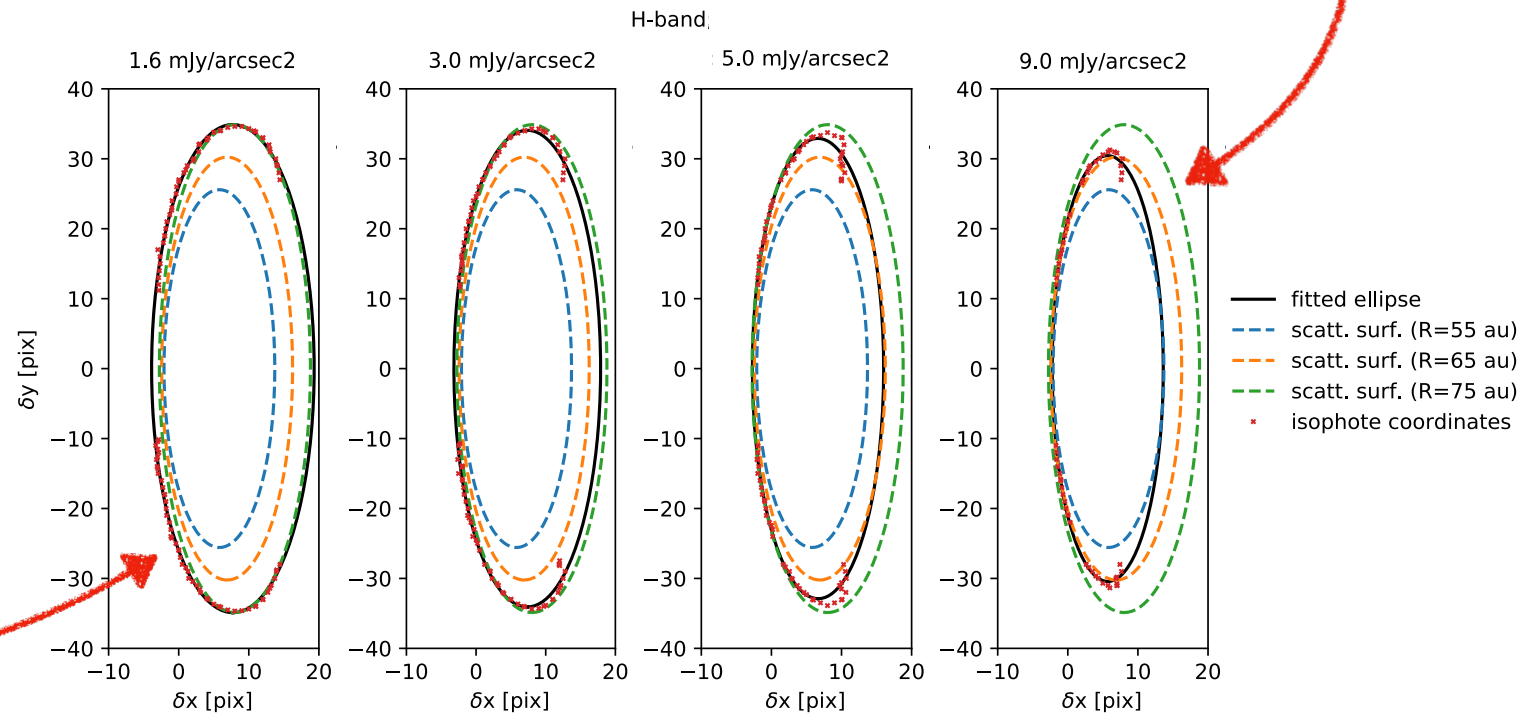

Stretched to the east close to the edge of the disc

Davies et al. (2021, *submitted*)

Summary

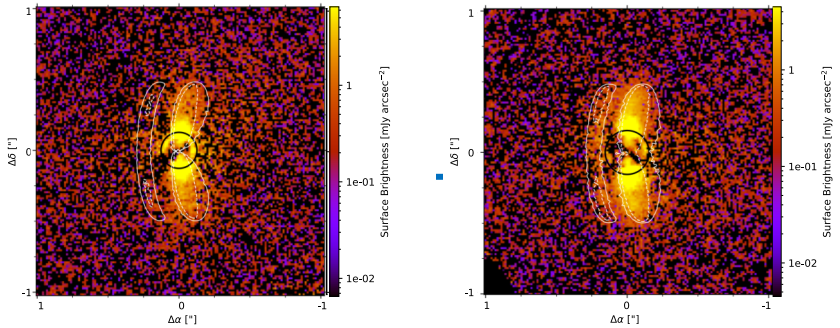

- G-LIGHTS observations of HD 145718, complemented with new and archival IR interferometry (CHARA+ VLTI) and archival spectro-photometry (use SEDBYS!)
- i = 67-71°, major axis PA = -1.0 – +0.6°, $R_{out} \approx 75$ au, $h_{scat}(r)/r$ = 0.13 – 0.16 (J-band) and 0.10 – 0.13 (H-band)
- Apparent evidence that grains > $\lambda/2\pi$ are present in the surface layers of the disc and grains > 0.50 µm have settled:
  - Scattering phase function (``pacman-like" feature in the Q_ϕ images)
  - Shape of the sublimation rim
  - Consistent values of $L_\star$ found when using R_v = 3.1 with bright-epoch and R_v = 5.0 with faint-epoch photometry
- If the inclination can be independently constrained (using e.g. ALMA), can use isophote fitting method on similarly inclined, apparently full discs to probe the flaring of the scattering surface.

Davies et al. (2021, *submitted*)